

Journal of Medical Sciences

ISSN 1682-4474





ISSN 1682-4474 DOI: 10.3923/jms.2022.128.139



Research Article Fraxetin with Low Dose Methotrexate Ameliorates Pristane-Induced Arthritis in Rats: Histological and Immunohistochemical Study

Samah Kandeel

Department of Histology and Cell Biology, Faculty of Medicine, Tanta University, Tanta 31527, Egypt

Abstract

Background and Objective: Pristane-Induced Arthritis (PIA) is a model of rheumatoid arthritis with a chronic relapsing course. Fraxetin (FXT) is a natural coumarin with antioxidant, anti-inflammatory and antifibrotic properties. This research evaluated the ameliorating effect of fraxetin with low dose Methotrexate (MTX) of PIA in rats. **Materials and Methods:** The 80 (100-200 g) Lewis female rats (8-10 weeks) divided into eight groups (10 rats each), group 1 (control), group 2 (vehicle): Rats received 0.5% CMC (carboxymethyl cellulose), group 3 (Pristane-induced arthritis (PIA)): Rats received an intradermal injection of 150 μL pristane oil, group 4 (PIA+MTX LD): PIA rats received low dose MTX (1 mg/kg/day) orally, group 5 (PIA+FXT LD): PIA rats received low dose fraxetin (25 mg/kg/day) orally, group 6 (PIA+FXT HD): PIA rats received high dose of fraxetin (50 mg/kg/day) orally, group 7 (PIA+FXT LD+MTX LD): PIA rats received low dose MTX and group 8 (PIA+FXT HD+MTX LD): PIA rats received high dose fraxetin plus low dose MTX orally. Treatments started from day 4 after PIA injection till the end of week 8. Knee joint specimens were processed for histopathology and immunohistochemistry. **Results:** Group 3 showed significantly increased total and differential leukocyte count, articular erosions, synovial inflammatory infiltrations, significantly reduced articular cartilage width, significantly decreased periodic acid-Schiff, significantly increased mean collagen area percent, significantly increased TGF-β1(anti-transforming growth factor-β1) stained synovial fibroblasts. The PIA groups treated with MTX and FXT exhibited a dose-dependent reduction of the previous findings. **Conclusion:** FXT dose-dependent with low dose MTX ameliorates PIA in rats.

Key words: Fraxetin, histopathology, immunohistochemistry, pristane, rats, rheumatoid arthritis

Citation: Kandeel, S., 2022. Fraxetin with Low dose methotrexate ameliorates pristane-induced arthritis in rats: Histological and immunohistochemical study. J. Med. Sci., 22: 128-139.

Corresponding Author: Samah Kandeel, Department of Histology and Cell Biology, Faculty of Medicine, Tanta University, Tanta 31527, Egypt

Copyright: © 2022 Samah Kandeel. This is an open access article distributed under the terms of the creative commons attribution License, which permits unrestricted use, distribution and reproduction in any medium, provided the original author and source are credited.

Competing Interest: The author has declared that no competing interest exists.

Data Availability: All relevant data are within the paper and its supporting information files.

INTRODUCTION

Rheumatoid Arthritis (RA) is a chronic systemic autoimmune disease with a prevalence rate of approximately 0.5-1% in adults in developed countries. It affects mainly the synovial lining of peripheral joints and causes joint inflammation, cartilage and bone destruction, which subsequently results in joint deformation and disability. Extra-articular manifestations including keratitis, pulmonary rheumatoid nodules and small-vessel vasculitis may occur under poorly controlled and/or severe conditions. It has been suggested that RA is caused by environmental factors combined with a genetic predisposition however, the pathogenesis of RA remains poorly defined. Diagnosis of RA depends on clinical manifestations including joint swelling with redness and morning joint stiffness¹.

Pristane-induced arthritis (PIA) is an animal model of RA using pristane mineral oil. Pristane is a natural component in plants that can be ingested and absorbed by the intestine of rats and humans. PIA produces early onset of RA. Injection of pristane in rats causes the chronic relapsing course of arthritis with symmetrical joint manifestations, cartilage and bone destruction as well as the associated appearance of rheumatoid factor. PIA is a preferred rat model for studying arthritis as it demonstrates the long term effects of immune-inflammatory processes. So, its joint manifestations could resemble the human RA^{2,3}.

There is no cure for RA, current treatments reduce disease activity, by preventing or controlling joint damage and also the other extra-articular manifestations. So, by early intervention, the joint function can be preserved. Methotrexate (MTX) is an anti-folate drug whose mechanism of action includes inhibition of dihydrofolate reductase (DHFR). It has been used for treating cancer, it also is used for treating RA, MTX treatment is limited owing to its systemic side effects, especially at high doses. MTX at low doses reduces ATP and GTP levels, reduces T cell proliferation and the increased T cell apoptosis, however low doses may not reduce RA⁴.

Alternative RA treatments are expensive. Therefore, other immunomodulatory and anti-inflammatory drugs with low organ toxicity are required. Combinations of immunomodulatory and anti-inflammatory drugs with a low dose of MTX produce better results than using a single drug alone⁵.

Fraxetin (FXT) is a natural coumarin derivative widely distributed in natural plants, like citrus fruits, tomatoes, vegetables as well as green tea. It is extracted from Cortex fraxini and exhibits antioxidant, anti-inflammatory and

antifibrotic properties. It protects the cells by decreasing the release of inflammatory cytokines including TNF- α , TGF- β 1 and IL-1 β and by decreasing apoptosis of osteoblasts. Consequently, FXT can be used to treat inflammatory diseases^{6,7}.

This research investigated the ameliorative effects of combination therapy using different doses of FXT with low dose MTX for treating RA using a rat model of RA produced by pristane.

MATERIALS AND METHODS

Study area: This study was done during the year 2020.

Animals: The experiment was conducted following the guidelines of Tanta University for the care and use of experimental animals with the approval of the University Animal Experiment Committee (Approval Code. 34302/12/20). We used 80 (100-200 g) lewis female rats (8-10 weeks) obtained from the animal house, Faculty of Medicine, Tanta University, Egypt. The animals were housed in pathogen-free clean plastic cages, at ($22\pm1\,^{\circ}$ C) and $60\pm5\%$ relative humidity with a 12 hrs light: 12 hrs dark cycles. The animals were fed a standard laboratory diet and water *ad libitum*.

Induction of PIA: PIA was induced according to the previously published methodologies, using a single intradermal injection of 150 μ L pristane mineral oil (2, 6, 10, 4-tetramethylpentadecane, Sigma-Aldrich, Egypt) at the base of the rat tail³.

Preparation of MTX: MTX (Pfizer Pharmaceuticals Ltd., Cairo, Egypt) was dissolved in 0.5% CMC (carboxymethyl cellulose). MTX is administered to rats daily by intragastric gavage⁸.

Preparation of FXT: FXT was prepared according to earlier reports. FXT powder (Sigma-Aldrich, Egypt) was dissolved in distilled water at two doses and administered by gastric lavage, a low dose fraxetin (FXT LD) was given at a dose of 25 mg/kg/day and a high dose (FXT HD) of 50 mg/kg/day¹⁶.

Experimental groups: Rats were divided into eight groups of (10 rats each):

- **Group 1 (control group):** Was subdivided into five untreated rats and five rats were administered distilled water orally in an amount corresponding to FXT
- Group 2 (vehicle group) (VEH): Were administered 0.5%
 CMC orally in a volume corresponding to the MTX dose

- **Group 3 (PIA):** Were administered a single intradermal injection of 150 µL pristane
- **Group 4 (PIA+MTX LD):** PIA rats were administered 1 mg/kg/day MTX low dose orally
- Group 5 (PIA+FXT LD): PIA rats were administered
 25 mg/kg/day FXT low dose orally
- **Group 6 (PIA+FXT HD):** PIA rats were administered 50 mg/kg/day FXT high dose orally
- Group 7 (PIA+FXT LD+MTX LD): PIA rats were administered low dose FXT+low dose MTX
- Group 8 (PIA+FXT HD+MTX LD): PIA rats were administered high dose FXT+low dose MTX

The oral doses were given through an intragastric tube. All treatments were begun on day 4 of the experiment after PIA induction until the end of week 8. Rats were sacrificed by cervical dislocation. Then, synovial fluid lavage and knee joint specimens were obtained and processed for histopathological and immunohistochemical evaluation.

Synovial fluid lavage: Synovial fluid was examined using methods reported earlier. Rats were anesthetized using 0.25 mL kg⁻¹ 2:1 ketamine/xylazine. Under aseptic conditions, the knee joint was flexed 30°C and the synovial fluid was obtained through a small incision in the area directly above the patella. A needle was introduced into the synovial cavity and 25 mL saline containing EDTA was injected. Fluid withdrawal using a second needle inserted into the synovial cavity approximately 3 mm from the infusion needle^{9,10}.

Total as well as differential leukocytes, were counted manually using a haemocytometer microscope (Tokyo, Japan) by which the cell pellets were stained by Trypan blue. The formula of (cell \times 10³ mm⁻³ of synovial fluid) was used¹⁰.

Histopathological study: Joint specimens were decalcified with 10% buffered EDTA, then serial sagittal sections of 5 μ m were obtained including epiphyses and diaphysis¹¹.

Hematoxylin and eosin (H and E) staining: After deparaffinization, sections were rehydrated through descending alcohols, then stained with hematoxylin for 10 min, followed by counterstaining with a 1% solution of eosin for 10 min. Finally, sections were dehydrated, cleared and mounted in Canada balsam¹¹.

Arthritis in H and E stained sections was scored 0, no pathology, 1, mild articular cartilage degeneration with no inflammatory cells, 2, moderate articular cartilage degeneration with synovial membrane hyperplasia, pannus formation and a moderate number of inflammatory cells, 3,

severe articular cartilage degeneration with pannus formation and the large number of inflammatory cells. Slide reviewers were blinded to the identity of the sections¹².

Morphometric analysis of the width of the articular cartilage (mm) was measured using H and E stained sections. Leica Q500 MCO analyzer (Tokyo, Japan) was used measurements were made at the middle of the articular cartilage. Ten randomly selected fields were measured at ×400 using ten sequential sections from ten different specimens of each experimental group.

Periodic Acid Schiff (PAS) staining: Sections were deparaffinized, rehydrated, then immersed in 1% periodic acid. Sections were placed in Schiff's reagent for 15 min, then washed with tap water for 5 min. Sections were dehydrated with ascending alcohols, cleared with xylol and mounted in Canada balsam¹¹. The optical density of PAS stained articular sections (i.e., optical density (absorbance) is the material's ability to absorb the power of a given light which is passed through that material) was evaluated by using an image analysis system (Leica Q 500 MC) (Tanta Research Center, Faculty of Medicine). For each specimen, ten randomly selected microscopic fields from ten different specimens for each group were assessed at ×100.

Mallory's trichrome stain: Sections were deparaffinized, rehydrated and washed in distilled water. This followed by, re-fixation in Bouin's solution and stained with Wiegert's iron hematoxylin. Then, with Biebrich scarlet-acid fuchsine solution. After that, sections were differentiated in the phosphotungstic acid solution until the collagen is not red then, situated directly in aniline blue stain followed by differentiation with 1% acetic acid solution. Finally, sections were dehydrated and cleared in xylene¹¹. The mean area percentage of collagen in Mallory's trichrome stained sections was determined using a Leica Q 500 MC. Ten microscopic fields from ten specimens from each group were measured at ×100.

Immunohistochemistry of TGF-β1 (anti-transforming growth

factor- beta1): Sections were deparaffinized and rehydrated, then placed in 0.3% hydrogen peroxide/methanol for 20 min to block the endogenous peroxidase activity. Sections were heated for 5 min in a microwave oven, then left to cool followed by the addition of a serum-free protein blocking solution for 20 min. Sections then were incubated overnight at 4°C with anti-TGF-β1 antibody (Santa Cruz Biotechnology, USA) (diluted 1:200). Sections were washed with PBS buffer and incubated with the biotinylated goat anti-rabbit secondary antibody (Vector Labs, Peterborough, UK) (diluted

1:200) for 10 min at room temperature. One or two drops of DAB (3,3'-diaminobenzidine) were applied to the sections for 5-10 min then, counterstained with Mayer's hematoxylin, dehydrated, cleared and examined using a light microscope (Olympus, Tokyo, Japan)¹³. TGF- β 1 appeared brown in the cytoplasm of synovial fibroblasts. The primary antibody was replaced by PBS for the negative control. Also, the spleen is considered as a positive control for TGF- β 1. The number of TGF- β 1 stained synovial fibroblasts was counted using an Image J software program (Java 1.6.1. 2017. NIH, Bethesda, MD). Ten photographs from each experimental group at \times 400 were evaluated.

Statistical analysis: Minitab Statistical Software for Windows (version 16.1, Minitab Inc., State College, PA, USA) was used for statistical analysis. Variance of data were analyzed using either two-tailed Student's t-test or the Mann-Whitney's U-test after the evaluation of the F-test to compare between groups 2,3 with group 1, and one-way ANOVA test to compare between groups 4,5,6,7,8 with group 3. Values for P = 0.05 were considered significant.

RESULTS

Synovial fluid total and differential leukocyte count: The total leukocyte count (neutrophils, lymphocytes, and monocytes) for group 3 (PIA) showed a significant increase in group 3 (group 3, 6.9) compared to group 1 (control) (group 1, 0.7). Conversely, group 4 (group 4, 0.9) as well as groups 5 (group 5, 3.5), 6 (group 6, 2.6), 7 (group 7, 1.7) and 8 (group 8, 1.1) exhibited a significant decrease in the total leukocyte count compared to group 3 in Fig. 1. Neutrophils count showed a significant increase in group 3 (group 3, 0.72) compared to group 1 (control) (group1, 0.62). Conversely, group 4 (group 4, 0.58) as well as groups 5 (group 5, 0.52), 6 (group 6, 0.45), 7 (group 7, 0.41) and 8 (group 8, 0.36) exhibited a significant decrease in neutrophils count compared to group 3 in Fig. 2. Lymphocytes count showed a significant increase in group 3 (group 3, 3) compared to group 1 (control) (group 1, 0.82). Conversely, group 4 (group 4, 0.71) as well as groups 5 (group 5, 2.31), 6 (group 6, 1.5), 7 (group 7, 1.22) and 8 (group 8, 0.92) exhibited a significant decrease in lymphocytes count compared to group 3 in Fig. 3. Also, monocytes count showed a significant increase in group 3 (group 3, 3.5) compared to group 1 (control) (group 1, 0.6). Conversely, group 4 (group 4, 0.5) as well as groups 5 (group 5, 3), 6 (group 6, 2.8), 7 (group 7, 2.4) and 8 (group 8, 1.8) exhibited a significant decrease in monocytes count compared to group 3 in Fig. 4.

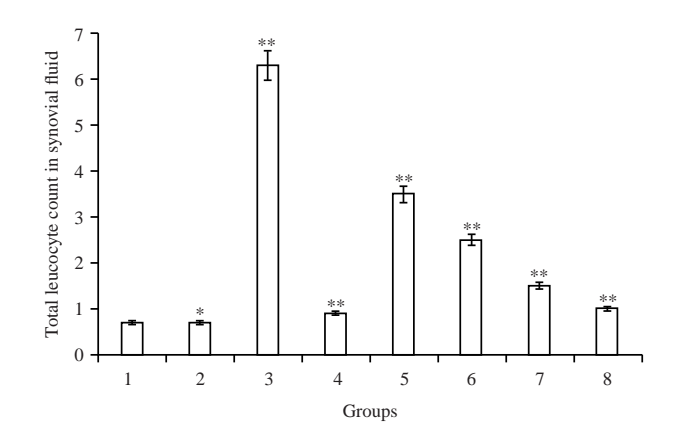


Fig. 1: Effect of different doses of FXT with low dose MTX on the synovial fluid (SF) total leucocyte count of PIA in rats

Data are Means \pm SD, *Group 2 (vehicle), p>0.05 compared to group 1 (control), **Group 3 (PIA), p<0.05 compared to group 1 and groups 4 (PIA+MTXLD), 5 (PIA+FXTLD), 6 (PIA+FXTHD), 7 (PIA+FXTLD+MTXLD) and 8 (PIA+FXT HD+MTX LD) p<0.05 compared to group 3

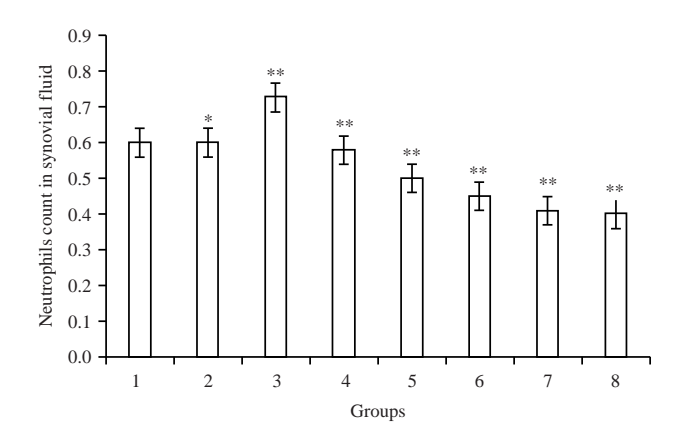
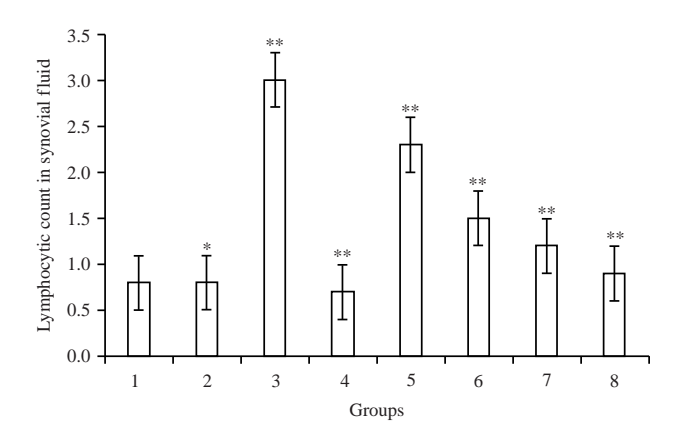


Fig. 2: Effect of different doses of FXT with low dose MTX on the synovial fluid (SF) neutrophils count of PIA in rats Data are Means±SD, *Group 2 (vehicle), p>0.05 compared to group 1 (control), **Group 3 (PIA), p<0.05 compared to group 1 and groups 4 (PIA+MTXLD),5 (PIA+FXTLD),6 (PIA+FXTHD),7 (PIA+FXTLD+MTXLD) and 8 (PIA+FXT HD+MTXLD) p<0.05 compared to group 3

H and E results: H and E stained sections from groups 1 and 2 exhibited smooth articular surface and no perichondrium, with normal synovial tissue containing adipocytes. The articular cartilages were basophilic and consisted of a superficial smooth surface and four dissimilar zones of chondrocytes, a superficial zone with flattened chondrocytes, a transitional zone composed of scattered and larger chondrocytes, a radial zone, containing rows of chondrocytes, a zone of calcified cartilage that separated the radial zone from the underlying subchondral bone and contained scattered chondrocytes in Fig. 5a and b. Group 3 exhibited



4.5 4.0 Monocytic count in synovial fluid 3.5 3.0 2.5 2.0 1.5 1.0 0.5 0.0 7 2 3 5 6 Groups

Fig. 3: Effect of different doses of FXT with low dose MTX on the synovial fluid (SF) lymphocytes count of PIA in rats Data are Means±SD, *Group 2 (vehicle), p>0.05 compared to group 1 (control), **Group 3 (PIA), p<0.05 compared to group 1 and groups 4 (PIA+MTX LD), 5 (PIA+FXT LD), 6 (PIA+FXT HD), 7 (PIA+FXT LD+MTX LD) and 8 (PIA+FXT HD+MTX LD) p<0.05 compared to group 3

Fig. 4: Effect of different doses of FXT with low dose MTX on the synovial fluid (SF) monocytes count of PIA in rats Data are Means±SD, *Group 2 (vehicle), p>0.05 compared to group 1 (control), **Group 3 (PIA), p<0.05 compared to group 1 and groups 4 (PIA+MTXLD), 5 (PIA+FXTLD), 6 (PIA+FXTHD), 7 (PIA+FXTLD+MTXLD) and 8 (PIA+FXT HD+MTXLD) p<0.05 compared to group 3

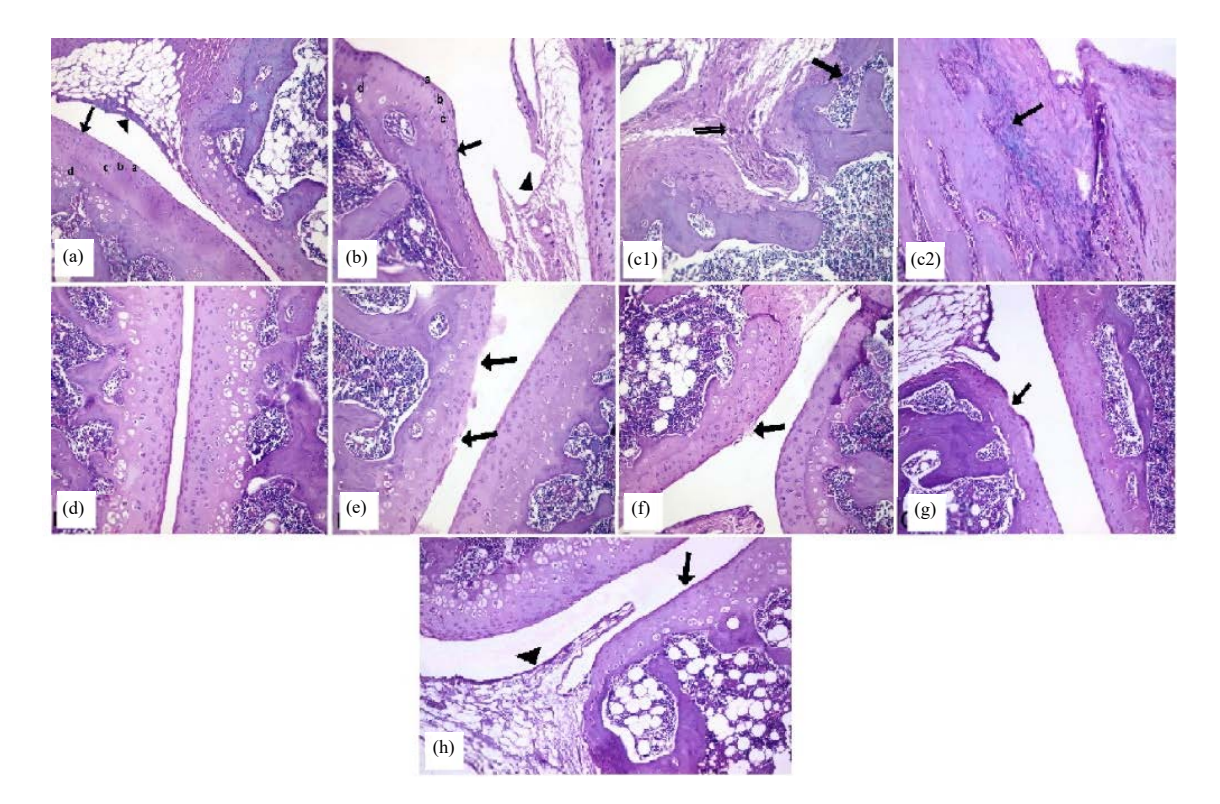
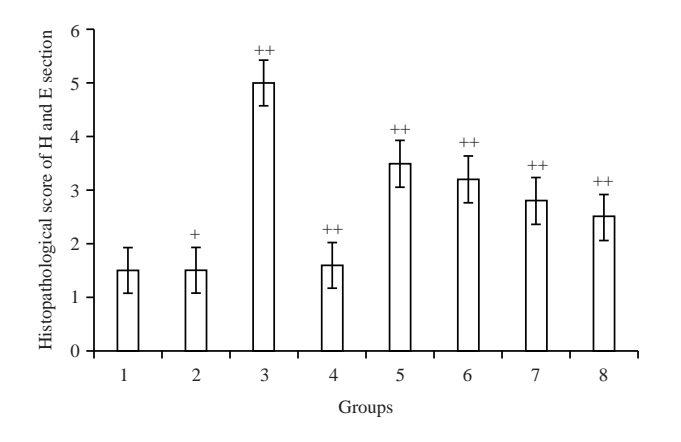


Fig. 5(a-h): Effect of different doses of FXT with low dose MTX by H and E staining of PIA in rats, (a, b) Groups 1 and 2 respectively: Smooth articular surface with no perichondrium (→), normal synovial tissue containing adipocytes (►), superficial zone with flattened chondrocytes (a), transitional zone with scattered and larger chondrocytes (b), radial zone with rows of chondrocytes (c), zone of calcified cartilage containing scattered chondrocytes (d). (c1) Group 3: Articular surface erosions (→), synovial tissue invaded the joint cavity and the articular surface (double arrows). (c2) inflammatory cell infiltrations (→). (d) Group 4: nearly normal articular joint. (e) Group 5 with multiple areas of surface erosion (→). (f) Group 6 with an area of surface erosion (→). (g) Group 7 showing a small area of articular surface erosion (→). (h) Group 8 shows smooth articular surface (→) and nearly normal synovial tissue (►) H and E (x400).



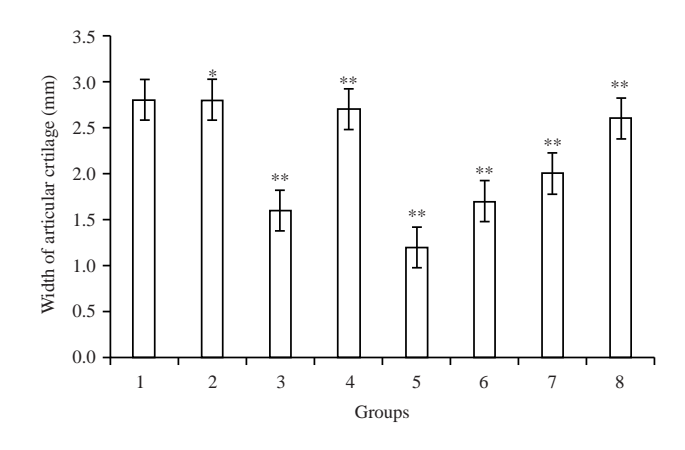


Fig. 6: Effect of different doses of FXT with low dose MTX on the histopathological scoring of H and E stained sections of PIA in rats

Data are Means \pm SD, $^+$ Group 2 (vehicle), p>0.05 compared to group 1 (control), $^{++}$ Group 3 (PIA), p<0.05 compared to group 1 and groups 4 (PIA+MTX LD), 5 (PIA+FXT LD), 6 (PIA+FXT HD), 7 (PIA+FXT LD+MTX LD) and 8 (PIA+FXT HD+MTX LD) p<0.05 compared to group 3

Fig. 7: Effect of different doses of FXT with low dose MTX on the articular cartilage' width of PIA in rats

Data are Means \pm SD, *Group 2 (vehicle), p>0.05 compared to group 1 (control), **Group 3 (PIA), p<0.05 compared to group 1 and groups 4 (PIA+MTX LD), 5 (PIA+FXT LD), 6(PIA+FXT HD), 7 (PIA+FXT LD+MTX LD) and 8 (PIA+FXT HD+MTX LD) p<0.05 compared to group 3

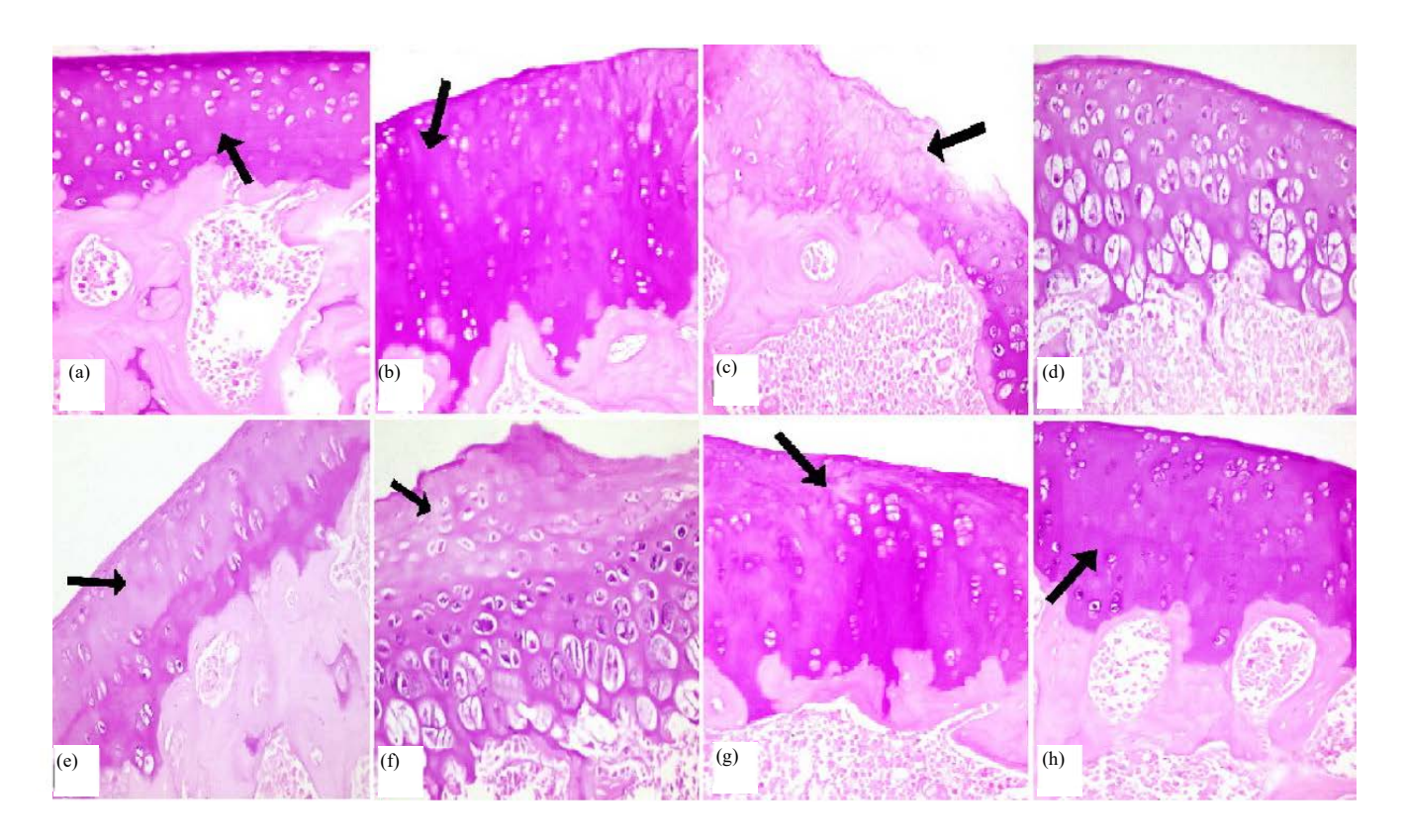


Fig. 8(a-h): Effect of different doses of FXT with low dose MTX on PAS staining of PIA in rats. (a, b) Groups 1 and 2 respectively: strong PAS staining of articular matrix (→). (c) Group 3: decreased staining of articular matrix (→). (d) Group 4: nearly normal PAS staining. (e) Group 5: decreased PAS staining of articular matrix (→). (f) Group 6: decreased PAS staining of articular matrix (→). (g) Group 7: an area with decreased PAS staining of articular matrix (→). (h) Group 8: nearly normal PAS staining (→) PAS (x 400)

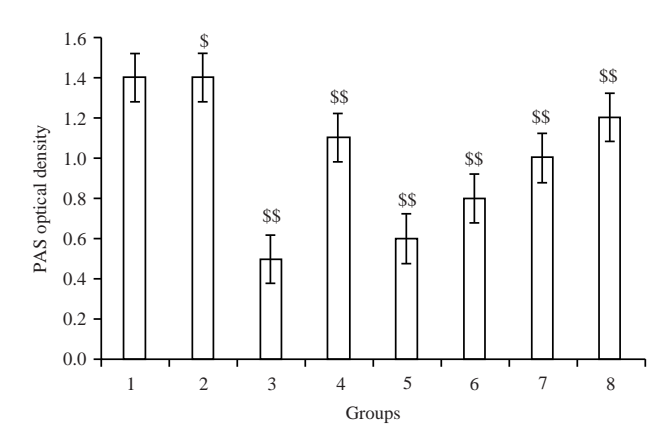


Fig. 9: Effect of different doses of FXT with low dose MTX on articular PAS staining of PIA in rats

Data are Means ± SD, \$Group 2 (vehicle), p>0.05 compared to group 1 (control), \$Group 3 (PIA), p<0.05 compared to group 1 and groups 4 (PIA+MTX LD), 5 (PIA+FXT LD), 6 (PIA+FXT HD), 7 (PIA+FXT LD+MTX LD) and 8 (PIA+FXT HD+MTX LD) p<0.05 compared to group 3

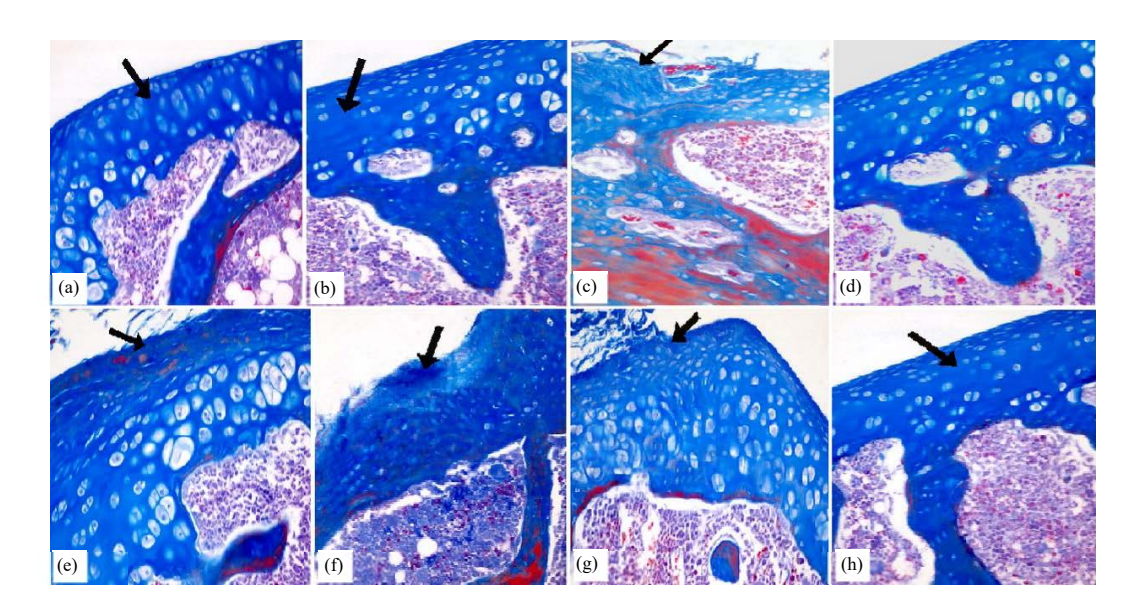


Fig. 10(a-h): Effect of different doses of FXT with low dose MTX on Mallory's trichrome staining of PIA in rats, (a, b) Groups 1 and 2 respectively: smooth articular cartilage with regular staining affinity of the articular matrix for collagen fibers (→). (c) Group 3: a layer of collagen fibers covering the eroded articular surface (→). (d) Group 4: smooth articular cartilage. (e) Group 5: an irregular wide area of collagen fibers covering the articular surface (→). (f) Group 6: an area of collagen fibers covering the eroded surface with irregularity (→). (g) Group 7: an area of collagen fibers covering the articular surface (→). (h) Group 8: regular staining affinity of the articular matrix for collagen fibers (→) Mallory's trichrome (x 400).

areas of articular surface erosions and irregularities. Also, the synovial tissue invaded the joint cavity and intruded on the articular surface accompanied by inflammatory cellular infiltrations (i.e., pannus) in Fig. 5c1 and c2. Nearly normal histology was observed in group 4 with nearly normal articular joint and synovial tissue in Fig. 5d. Group 5 exhibited multiple surface erosions by contrast to a focal area of surface erosion in group 6 in Fig. 5e and f, respectively).

Group 7 exhibited a focal area of an articular surface erosion with nearly normal synovial tissue, compared to group 8, which exhibited improvement with preserved smooth articular surface and nearly normal synovial tissue similar to the control group in Fig. 5g and h, respectively.

Statistically, significantly increased histopathological scoring in group 3 (group 3, 5) was seen compared to group 1 (group 1, 1.5). Group 4 showed significantly decreased

histopathological score (group 4, 1.6) compared to group 3. Also, groups 5 (group 5, 3.5), 6 (group 6, 3.2), 7 (group 7, 2.8) and 8 (group 8, 2.5), respectively showed significant decrease compared to group 3 (PIA group) in Fig. 6.

A significant decrease of the articular cartilage' width in group 3 compared to group 1 was observed. While, significantly increased in group 4 as well as in groups 5, 6, 7 and 8, respectively compared to group 3 in Fig. 7.

PAS results: PAS stained sections from groups 1 and 2 exhibited strong PAS staining of the articular matrix in Fig. 8a and b. In group 3, the staining of the articular matrix decreased in Fig. 8c. In group 4 nearly normal histology was observed by contrast to many areas of decreased PAS-staining affinity in groups 5 and 6 in Fig. 8d-f. In group 7, found a focus with decreased staining of the articular matrix by contrast to nearly normal staining in group 8 in Fig. 8g and h.

The optical density (absorbance) for PAS stained sections exhibited a significant decrease in PAS staining in group 3 (group 3, 0.5) compared to group 1 (group 1, 1.4). In PIA groups, the optical density (absorbance) of PAS stained sections exhibited a significant increase in group 4 (group 4, 1.1) as well as in groups 5 (group 5, 0.5), 6 (group 6, 0.8), 7 (group 7, 1) and 8 (group 8, 1.2) in a dose-dependent manner compared to group 3 in Fig. 9.

Mallory's trichrome results: Mallory's trichrome stained sections from group 1 and 2 exhibited smooth articular cartilage with blue staining of collagen fibres in the articular matrix in Fig. 10a and b. In group 3, the articular cartilage exhibited an irregular layer of collagen fibres covering the

eroded surface in Fig. 10c, whereas, group 4 exhibited nearly normal staining with smooth articular cartilage in Fig. 10d. Conversely, group 5 showed an irregular area of collagen fibres covering the articular surface in Fig. 10e, while a layer of blue collagen fibres covering the eroded surface was found in group 6 in Fig. 10f. Group 7 exhibited an area of dark blue collagen fibres covering the articular surface in Fig. 10g by contrast to the nearly normal appearance in group 8 in Fig.10h.

The mean area percentage of the articular collagen fibres was significantly increased in group 3 (group 3, 3) compared to group 1 (group 1, 1). In the PIA groups, there was a significant decrease in the mean area percentage of the articular collagen fibres in group 4 (group 4, 1.1) as well as in groups 5 (group 5, 2), 6 (group 6, 1.5), 7 (group 7, 1.2) and 8 (group 8, 0.8) dose-dependently compared to group 3 in Fig. 11.

TGF-β1 immunohistochemical results: The negative control showed no TGF-β1 immunohistochemical expression of synovial fibroblasts in Fig. 12a. Few synovial fibroblasts were immunostained for TGF-β1 in group 1 and 2 in Fig. 12b and c. In group 3, increased numbers of synovial fibroblasts immunostained for TGF-β1 in Fig. 12d. Group 4 immunostaining was similar to the control in Fig. 12e. In group 5, most of the cells were immunostained for TGF-β1 in Fig. 12f. In contrast, only some cells were immunostained for TGF-β1 in group 6 in Fig. 12g. In group 7 a few cells were immunostained for TGF-β1 in Fig.12h, whereas, in group 8, a nearly normal TGF-β1 immunohistochemical reaction was found in Fig. 12i.

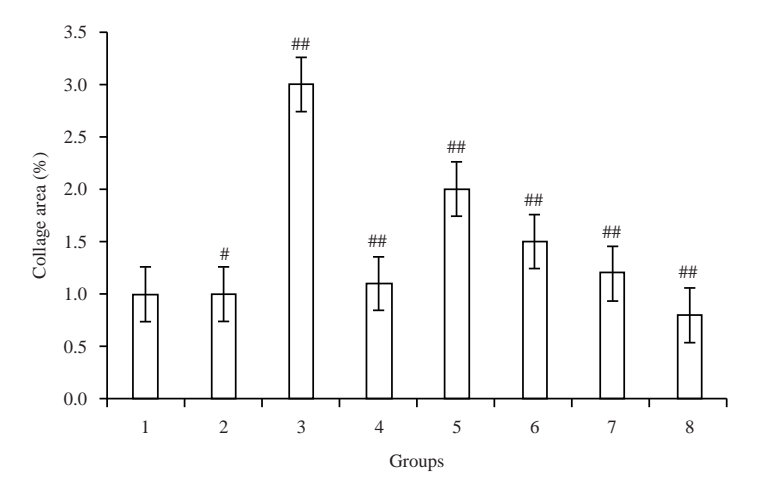


Fig. 11: Effect of different doses of FXT with low dose MTX on mean area percentage of articular collagen fibers of PIA in rats

Data are Means ±SD, *Group 2 (vehicle), p>0.05 compared to group 1 (control), *Group 3 (PIA), p<0.05 compared to group 1 and groups 4 (PIA+MTX LD),

5(PIA+FXT LD), 6 (PIA+FXT HD), 7 (PIA+FXT LD+MTX LD) and 8 (PIA+FXT HD+MTX LD) p<0.05 compared to group 3

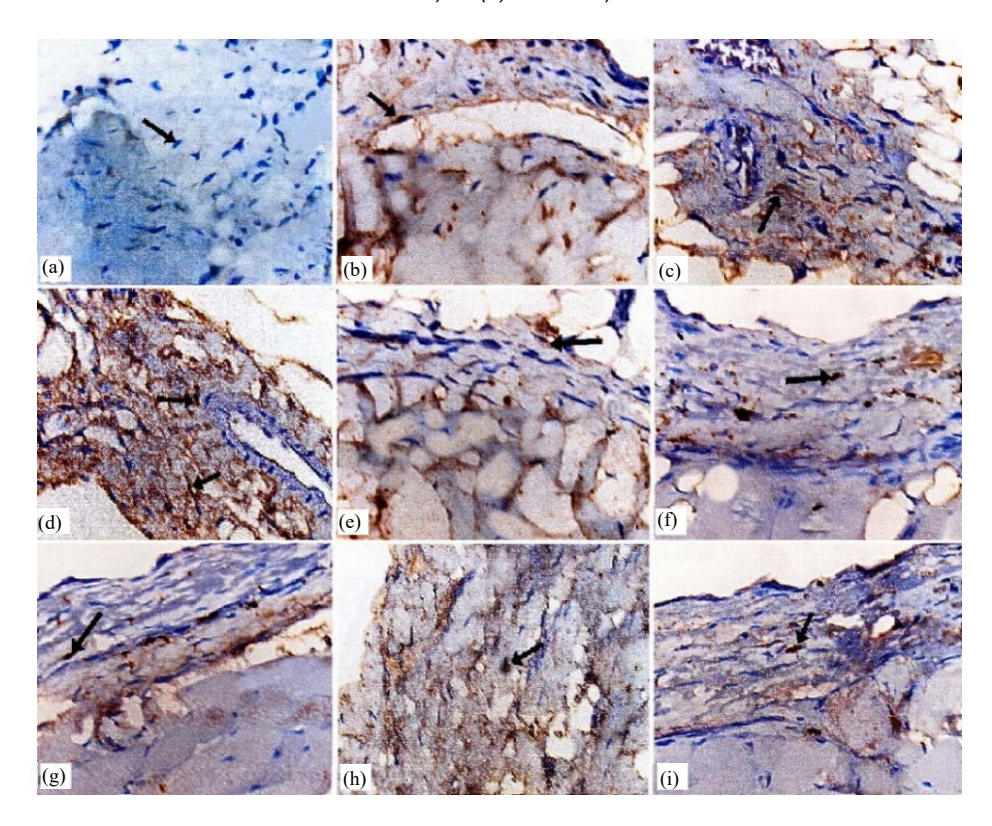


Fig. 12(a-i): Effect of different doses of FXT with low dose MTX on TGF- β 1 immunostaining of synovial fibroblasts of PIA in rats, (a) Negative control: No TGF- β 1 immunohistochemical expression of synovial fibroblasts (\rightarrow). (b, c) Groups 1 and 2 respectively: little synovial fibroblasts with positive immunostaining for TGF- β 1 (\rightarrow). (d) Group 3: most of the synovial fibroblasts showed positive TGF- β 1 immunostaining (\rightarrow). (e) Group 4: similar to control with little synovial fibroblasts with positive immunostaining for TGF- β 1 (\rightarrow). (f) Group 5: most of the synovial fibroblasts appeared with a positive immunostaining (\rightarrow). (g) Group 6: some cells appeared with a positive TGF- β 1 immunostaining (\rightarrow). (h) Group 7: few synovial fibroblasts appeared with a positive TGF- β 1 immunostaining (\rightarrow). (i) group 8: little cells with positive TGF- β 1 immunostaining (\rightarrow) TGF- β 1 immunostaining (\rightarrow). (TGF- β 1 immunostaining (\rightarrow) TGF- β 1 immunostaining (\rightarrow).

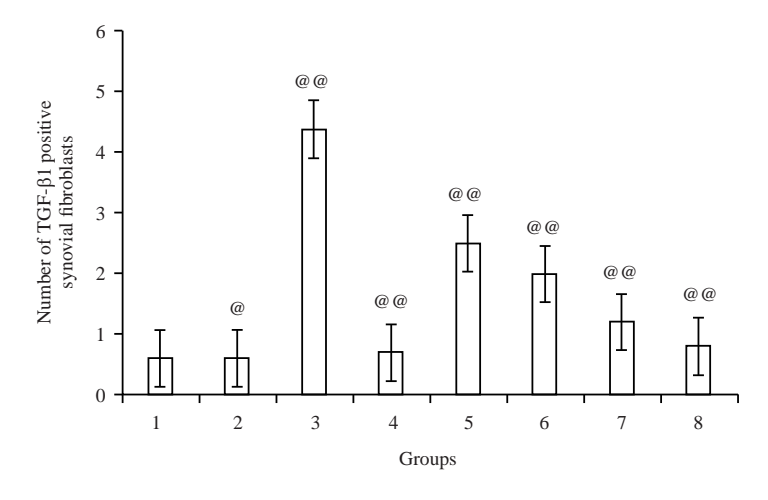


Fig. 13: Fig. 13. Effect of different doses of FXT with low dose MTX on the number of TGF-ß1 immunopositive synovial fibroblasts of PIA in rats.

Data are means \pm SD. (@): Group 2 (vehicle); P > 0.05 compared to group 1 (control). (@@): Group 3 (PIA); P < 0.05 compared to group 1 and groups 4 (PIA+MTX LD), 5 (PIA+FXT LD), 6 (PIA+FXT HD), 7 (PIA+FXT LD+MTX LD) and 8 (PIA+FXT HD+MTX LD) P < 0.05 compared to group 3.

The number of TGF- β 1 immunostained synovial fibroblasts was significantly increased in group 3 (group 3, 4.4) compared to group 1 (group 1, 0.6). While, a significant decrease in the number of TGF- β 1 immunostained synovial fibroblasts in group 4 (group 4, 0.7) as well as groups 5 (group 5, 2.5), 6 (group 6, 2), 7 (group 7, 1.2) and 8 (group 8, 0.8) compared to group 3, was seen in Fig. 13.

DISCUSSION

The present research revealed that PIA mimics human RA. H and E staining results for group 3 revealed a significant increase in the total as well as the differential leukocyte count including lymphocytes, monocytes and neutrophils. There were also articular surface erosions and synovial tissue invasion into the joint cavity and the articular surface. In addition to infiltrates of inflammatory cells (pannus) and significantly reduced articular cartilage' width. Other observations in group 3 were a significant decrease of the articular PAS staining affinity, a significant increase in the mean area percentage of articular collagen fibres, a significant increase in the number of synovial fibroblasts with the positive immunohistochemical reaction for TGF- β 1. These findings were consistent with those reported ¹³, who also asserted that the PIA model is preferable to other RA models.

The significantly increased total and differential leukocyte count in the synovial fluid as well as the articular surface erosions, pannus formation could be attributed to the role of synovial fibroblasts during inflammation. As synovial fibroblasts secrete pro-inflammatory cytokines including interleukin IL-1B. Consequently, tissue infiltration with a variety of immune cells including monocytes, neutrophils and lymphocytes. Cytokines cause the release of lysosomal enzymes and Matrix Metalloproteinases (MMPs) from synoviocytes and chondrocytes. Pro-inflammatory cytokines also stimulate the release of prostaglandin E2 and nitric oxide which initiate tissue inflammation. In addition, IL-1ß stimulates the secretion of TGF-β1 which causes cartilage degradation. Expansion of the synovial tissue occurs as a result of the formation of pannus that invades the articular cartilage, with subsequent destruction14.

The decreased PAS staining affinity of the articular cartilage in the present study could be attributed to the biomechanical dysfunction as well as cartilage destruction resulting from the matrix degradation enzymes produced by the synovial fibroblasts. These are including MMPs that cause disassembly of collagen type II¹⁵.

The present study showed significantly increased collagen content and increased expression of TGF-β1 in group 3.

TGF- β 1 is a growth factor that participates in the pathogenesis of arthritis, it is reported to be elevated during synovial inflammation as it stimulates the production of collagen through the stimulation of fibroblasts¹⁶. TGF- β 1 causes pro-inflammatory changes, including synovial membrane hyperplasia, inflammation and articular erosion. TGF- β 1 stimulates the secretion of interleukins, MMP-1, Connective tissue growth factor (CTGF) and platelet-derived growth factor (PDGF), which causes increased inflammatory cell infiltration into synovial tissue and synovial hyperplasia^{17,18}.

Increased inflammatory cellular infiltrations were related to the pathological findings in group 3. The activation of T-lymphocytes by pristane initiates the acute phase of arthritis followed by the chronic phase. Pristane exhibits no immunogenic properties so, it might be recognized by T or B lymphocytes. Moreover, the plasmacytoma-inducing capacity of pristane may depend on IL-6, an inflammatory cytokine that triggers the inflammatory reactions^{3,19}.

Also, in PIA, the non-digestible parts of pristane may be phagocytosed by macrophages. Subsequently, macrophages initiate the release of different pro-inflammatory cytokines including TGF- β 1 (factor induces fibrosis). This could stimulate T and B lymphocytes, followed by migration of lymphocytes to the joints to cause joint destruction^{20,21}.

The damaged cartilage will subsequently release antigens, resulting in further stimulation of T- lymphocytes and chronic immune stimulation. The cytokines released by pristane also may cause synovial hypertrophy with increased expression of the major histocompatibility complex II (MHC II), adhesion molecules and increased production of matrix components, which causes connective tissue fibrosis as demonstrated by Mallory's trichrome stain^{22,23}.

MTX is a standard drug for treating RA whose use has been limited by its side effects⁵. We investigated the use of low dose MTX with different doses of FXT as a therapy for RA patients. Current findings indicate an ameliorative effect of FXT on the histopathological characteristics of joints as seen in group 3, in a dose-dependent manner. The best results were obtained when a high dose of FXT was combined with a low dose MTX.

This is supported by the significant reduction of the total and differential leukocyte count, normal articular surface with significantly increased cartilage width in groups 4, 5, 6, 7 and 8 compared to group 3. Also in groups 4, 5, 6, 7 and 8, we found a significant reduction of the mean area percentage of articular collagen fibres using Mallory's trichrome stain, significantly increased PAS joint staining and a significant reduction of the number of TGF- β 1 immunostained synovial fibroblasts.

FXT is a coumarin derivative that is characterized by its antioxidative and anti-inflammatory effects. FXT exhibited anti-inflammatory and antifibrotic effects. It exhibits a protective effect on cells by decreasing the release of inflammatory cytokines including TGF- β 1, TNF- α and IL- $1\beta^{7,24}$. FXT reduces inflammation by inhibiting of production of soluble intercellular adhesion molecules (sICAM-1), which decreases leukocyte adhesion. Furthermore, FXT reduces MMP-1 expression in cartilage, which prevents cartilage degradation. FXT also inhibits the release of the proinflammatory 5-lipoxygenase and the cyclooxygenase pathways of the arachidonate metabolism of leucocytes, which decreases nitric oxide and prostaglandin E2 (PGE2) levels in the synovial fluid. It also inhibits the production of pro-inflammatory cytokines by macrophages. It also may produce its protective effect by increasing the release of the heme oxygenase 1 (HO-1) (a protein released in response to cell stress protecting cells from undergoing degradation and death)25-28.

CONCLUSION

It was found that FXT dose-dependent administration combined with low dose MTX ameliorates the histopathological findings of PIA in rats, through its anti-inflammatory and antifibrotic effects. So, FXT could is a promising option for treating RA.

SIGNIFICANCE STATEMENT

This study discovered that FXT can be beneficial for treating arthritis. Also, this study will help the researchers to uncover the critical areas of arthritis that many researchers were not able to explore. Thus a new theory on arthritis management may be arrived at.

REFERENCES

- Raafat, M.H., G.G. Hamam, M.S. Farhan, L.M. Sabbagh, N.M. Abeduldaem and A.M. Sharaf, 2018. Evaluation of the possible therapeutic role of omega-3 on ankle joint and lung in a model of rheumatoid arthritis in rats: A histological and immunohistochemical study. Egypt. J. Histol., 41: 250-263.
- 2. Cope, A.P., 2007. Arthritis Research: Methods and Protocols. Humana Press Inc., Totowa, New Jersy, ISBN: 9781597454025, Pages: 503.
- 3. Tuncel, J., S. Haag, M.H. Hoffmann, A.C.Y. Yau and M. Hultqvist *et al.*, 2016. Animal models of rheumatoid arthritis (I): Pristane-induced arthritis in the rat. PLoS ONE, Vol. 11. 10.1371/journal.pone.0155936.

- 4. Friedman, B. and B. Cronstein, 2019. Methotrexate mechanism in treatment of rheumatoid arthritis. Joint Bone Spine, 86: 301-307.
- Pašková, Ľ., V. Kuncírová, S. Poništ, D. Mihálová and R. Nosáľ *et al.*, 2016. Effect of n-feruloylserotonin and methotrexate on severity of experimental arthritis and on messenger RNA expression of key proinflammatory markers in liver. J. Immunol. Res., Vol. 2016. 10.1155/2016/7509653.
- Wu, B., R. Wang, S. Li, Y. Wang, F. Song, Y. Gu and Y. Yuan, 2019. Antifibrotic effects of fraxetin on carbon tetrachlorideinduced liver fibrosis by targeting NF-κB/IκBα, MAPKs and Bcl-2/Bax pathways. Pharmacol. Rep., 71: 409-416.
- 7. Kuo, P.L., Y.T. Huang, C.H. Chang and J.K. Chang, 2006. Fraxetin inhibits the induction of anti-Fas IgM, tumor necrosis factor- α and interleukin-1 β -mediated apoptosis by Fas pathway inhibition in human osteoblastic cell line MG-63. Int. Immunopharmacol., 6: 1167-1175.
- 8. Koyama, A., A. Tanaka and H. To, 2017. Daily oral administration of low-dose methotrexate has greater antirheumatic effects in collagen-induced arthritis rats. J. Pharm. Pharmacol., 69: 1145-1154.
- Zhi, L.Q., Q. Zhong, J.B. Ma, L. Xiao, S.X. Yao and X. Wang, 2020. LncRNA H19 inhibitor represses synovial cell proliferation and apoptosis in rats with rheumatoid arthritis via notch signaling pathway. Eur. Rev. Med. Pharmacol. Sci., 24: 7921-7921.
- Waseem, A., R.V.S. Pawaiya, D.D. Singh, K. Gururaj, N.K. Gangwar, V.K. Gupta and R. Singh, 2016. Cytological, microbiological and molecular evaluation of synovial fluid in natural cases of arthritis in Indian goats. Indian J. Vet. Pathol., 40: 210-214.
- 11. Suvarna, K., C. Layton and J. Bancroft, 2018. Bancroft's Theory and Practice of Histological Techniques. 8th Edn., Elsevier Health Sciences, US, ISBN: 9780702068645, Pages: 584.
- Tumurkhuu, G., S. Chen, E.N. Montano, D.E. Laguna and G. De Los Santos *et al.*, 2020. Oxidative DNA damage accelerates skin inflammation in pristane-induced lupus model. Front. Immunol., Vol. 11. 10.3389/fimmu.2020.554725.
- 13. Würgler-Hauri, C.C., L.M. Dourte, T.C. Baradet, G.R. Williams and L.J. Soslowsky, 2007. Temporal expression of 8 growth factors in tendon-to-bone healing in a rat supraspinatus model. J. Shoulder Elbow Surg., 16: S198-S203.
- 14. Cantley, M.D., M.D. Smith and D.R. Haynes, 2009. Pathogenic bone loss in rheumatoid arthritis: Mechanisms and therapeutic approaches. Int. J. Clin. Rheumatol., 4: 561-582.
- 15. Guo, Q., Y. Wang, D. Xu, J. Nossent, N.J. Pavlos and J. Xu, 2018. Rheumatoid arthritis: Pathological mechanisms and modern pharmacologic therapies. Bone Res., Vol. 6. 10.1038/s41413-018-0016-9.
- 16. Sutton, S., A. Clutterbuck, P. Harris, T. Gent and S. Freeman *et al.*, 2009. The contribution of the synovium, synovial derived inflammatory cytokines and neuropeptides to the pathogenesis of osteoarthritis. Vet. J., 179: 10-24.

- 17. Zhang, R.K., G.W. Li, C. Zeng, C.X. Lin and L.S. Huang *et al.*, 2018. Mechanical stress contributes to osteoarthritis development through the activation of transforming growth factor beta 1 (TGF-β1). Bone Joint Res., 7: 587-594.
- Neumann, E., S. Lefèvre, B. Zimmermann, S. Gay and U. Müller-Ladner, 2010. Rheumatoid arthritis progression mediated by activated synovial fibroblasts. Trends Mol. Med., 16: 458-468.
- Firestein, G.S., R.C. Budd, S.E. Gabriel, I.B. McInnes and J.R. BO'Dell, 2016. Kelley and Firestein's Textbook of Rheumatology. 10th Edn., Elsevier Health Sciences, US, ISBN: 9780323414944, Pages: 275.
- Zhang, L., R. Xing, Z. Huang, N. Zhang, L. Zhang, X. Li and P. Wang, 2019. Inhibition of synovial macrophage pyroptosis alleviates synovitis and fibrosis in knee osteoarthritis. Mediators Inflammation, Vol. 2019. 10.1155/2019/2165918.
- 21. Naik, S. and S. Wala, 2014. Arthritis, a complex connective and synovial joint destructive autoimmune disease: Animal models of arthritis with varied etiopathology and their significance. J. Postgraduate Med., 60: 309-317.
- 22. van den Berg, W.B., 2015. Animal models of arthritis. In: Rheumatology, Hochberg, M.C., J.S. Smolen, M.H. Weisman, A.J. Silman and M.E. Weinblatt (Eds.), Elsevier, Netherlands, ISBN: 978-0-323-09138-1, Pages: 743-749.

- 23. Yau, A.C.Y. and R. Holmdahl, 2016. Rheumatoid arthritis: Identifying and characterising polymorphisms using rat models. Dis. Models Mech., 9: 1111-1123.
- 24. Chen, X., X. Ying, W. Zhang, Y. Chen, C. Shi, Y. Hou and Y. Zhang, 2013. The hepatoprotective effect of fraxetin on carbon tetrachloride induced hepatic fibrosis by antioxidative activities in rats. Int. Immunopharmacol., 17: 543-547.
- Hadjipavlou-Litina, D.J., K.E. Litinas and C. Kontogiorgis, 2007. The anti-inflammatory effect of coumarin and its derivatives. Anti-Inflammatory Anti-Allergy Agents Med. Chem., 6: 293-306.
- 26. Kundu, J., I.G. Chae and K.S. Chun, 2016. Fraxetin induces heme oxygenase-1 expression by activation of Akt/Nrf2 or AMP-activated protein kinase α/Nrf2 pathway in HaCaT cells. J. Cancer Prev., 21: 135-143.
- Liang, C., W. Ju, S. Pei, Y. Tang and Y. Xiao, 2017. Pharmacological activities and synthesis of esculetin and its derivatives: A mini-review. Molecules, Vol. 22. 10.3390/ molecules22030387.
- 28. Chen, X., X. Ying, W. Sun, H. Zhu, X. Jiang and B. Chen, 2018. The therapeutic effect of fraxetin on ethanol-induced hepatic fibrosis by enhancing ethanol metabolism, inhibiting oxidative stress and modulating inflammatory mediators in rats. Int. Immunopharmacol., 56: 98-104.